Molecular Microbiology (2016) 101(4), 590–605 ■
doi:10.1111/mmi.13410
First published online 27 May 2016

A scaffold protein connects type IV pili with the Chp chemosensory system to mediate activation of virulence signaling in *Pseudomonas aeruginosa*

Yuki F. Inclan,[1] Alexandre Persat,[2] Alexander Greninger,[3] John Von Dollen,[4,5] Jeffery Johnson,[4,5] Nevan Krogan,[4,5,6] Zemer Gitai[2] and Joanne N. Engel[1,7]*

[1]*Department of Medicine, University of California, San Francisco, San Francisco, CA 94143, USA.*
[2]*Department of Biology, Princeton University, Princeton, NJ 08544, USA.*
[3]*Department of Biochemistry, University of California, San Francisco, San Francisco, CA 94143, USA.*
[4]*California Institute for Quantitative Biosciences, San Francisco, CA 94148, USA.*
[5]*Department of Cellular and Molecular Pharmacology, University of California, San Francisco, CA 94158, USA.*
[6]*Gladstone Institutes, San Francisco, CA 94158, USA.*
[7]*Department of Microbiology and Immunology, University of California, San Francisco, CA 94143, USA.*

Summary

Type IV pili (TFP) function as mechanosensors to trigger acute virulence programs in *Pseudomonas aeruginosa*. On surface contact, TFP retraction activates the Chp chemosensory system phosphorelay to upregulate 3′, 5′-cyclic monophosphate (cAMP) production and transcription of virulence-associated genes. To dissect the specific interactions mediating the mechanochemical relay, we used affinity purification/mass spectrometry, directed co-immunoprecipitations in *P. aeruginosa*, single cell analysis of contact-dependent transcriptional reporters, subcellular localization and bacterial two hybrid assays. We demonstrate that FimL, a Chp chemosensory system accessory protein of unknown function, directly links the integral component of the TFP structural complex FimV, a peptidoglycan binding protein, with one of the Chp system output response regulators PilG. FimL and PilG colocalize at cell poles in a FimV-dependent manner. While PilG phosphorylation is required for TFP function and mechanochemical signaling, it is not required for polar localization or binding to FimL. Phylogenetic analysis reveals other bacterial species simultaneously encode TFP, the Chp system, FimL, FimV and adenylate cyclase homologs, suggesting that surface sensing may be widespread among TFP-expressing bacteria. We propose that FimL acts as a scaffold enabling spatial colocalization of TFP and Chp system components to coordinate signaling leading to cAMP-dependent upregulation of virulence genes on surface contact.

Accepted 29 April, 2016. *For correspondence. E-mail jengel@medicine.ucsf.edu; Tel. +1 415-476-7355; Fax 415-476-9364.

Introduction

Pseudomonas aeruginosa is a versatile opportunistic pathogen found ubiquitously throughout the environment (Silby *et al.*, 2011). In susceptible human hosts, including immunocompromised patients, those with injury to the epithelial barrier or patients with cystic fibrosis (CF), *P. aeruginosa* can cause devastating disease (Mandell *et al.*, 2010). Not only is *P. aeruginosa* intrinsically resistant to multiple classes of antibiotics, it acquires antibiotic resistance readily (Livermore, 2002). As a result, multi- and extremely resistant strains are increasing in frequency, making development of new therapeutic approaches a critical need (Frieden, 2013).

By leveraging an uncommonly large number of sensing systems, *P. aeruginosa* can rapidly adapt to a wide variety of environments (Filloux and Ventre, 2006; Coggan and Wolfgang, 2012). Importantly, *P. aeruginosa* is particularly well armed to rapidly transition from swimming to surface associated states. It can grow planktonically, using flagellar mediated swimming motility to chemotax toward nutrients and away from toxins or predators. Alternatively, *P. aeruginosa* can switch to a sessile state by attaching to abiotic or biotic surfaces with flagella and/or with type IV pili (TFP) to initiate a

developmental program, including biofilm formation. In doing so, *P. aeruginosa* loses the ability to swim away from phagocytic predators, such as environmental amoeba or tissue neutrophils, but gains resistance to antimicrobials and to phagocytosis through inherent properties of the polysaccharide-encased multicellular biofilm. The planktonic lifestyle is usually associated with acute infections and toxicity mediated by the secretion of a large armamentarium of secreted virulence factors, including toxins injected into eukaryotic cells via the type III secretion system (T3SS) (Tolker-Nielsen, 2014). In contrast, the sessile, biofilm-associated state is associated with downregulation of secreted effectors and the development of chronic, highly antibiotic resistant infections, such as those that occur in the chronic, relentless and ultimately fatal lung infections specifically associated with CF patients (Tolker-Nielsen, 2014).

On binding to a biotic or abiotic surface, the transition between planktonic and sessile states is mediated by TFP (Tolker-Nielsen, 2014). These polarly localized fibers dynamically extend and retract by respective assembly and disassembly of pilin monomers encoded by *pilA* (Leighton *et al*., 2015). In addition to attachment, TFP powers locomotion over surfaces, also known as twitching motility, an essential feature of virulence and biofilm formation (Comolli *et al*., 1999; Leighton *et al*., 2015). A wide variety of genes are necessary for assembly and function of TFP (Leighton *et al*., 2015). These include structural and functional components including PilA and the retraction motor ATPase PilT, as well as regulatory components. For example, the Chp chemosensory system, a complex chemotaxis-like two-component system, is required for full surface pilin assembly and twitching motility (Whitchurch *et al*., 2004). More recently, we have shown that *P. aeruginosa* has the ability to regulate virulence on surface contact using TFP as mechanosensors that signal through the Chp chemosensory system (Persat *et al*., 2015a). However, the exact mechanism by which *P. aeruginosa* cells transduce the mechanical signal at the level of TFP into the Chp system phosphorelay response remains to be investigated.

The Chp system is composed of nine contiguous genes (PilG-K, ChpA-C) and one gene (FimL) encoded at a separate chromosomal locus (Whitchurch *et al*., 2004; Whitchurch *et al*., 2005; Bertrand *et al*., 2010; Inclan *et al*., 2011). Key components of the Chp system resemble those of typical chemosensory systems (Whitchurch *et al*., 2004). These include the presumptive chemoreceptor PilJ, a transmembrane Methyl-accepting Chemotaxis Protein MCP; ChpA, a hybrid CheA-like histidine kinase that encodes six histidine phosphotransfer (Hpt) domains and a C-terminal CheY-like receiver domain; and two additional CheY-like output response regulators PilG and PilH. FimL is an accessory protein of unknown function that has high homology to the N-terminus of ChpA, but lacks the residues and domains necessary for phosphorylation activity (Whitchurch *et al*., 2005). Based on similarity to the analogous chemosensory Che pathway that controls flagellar swimming motility (Baker *et al*., 2006), PilJ senses external signals and transduces a signal to ChpA. ChpA undergoes autophosphorylation at one or more of the conserved histidines and then transfers the phosphoryl group to one of three potential receiver domains, the CheY domain of ChpA or the separately encoded response regulators, PilG and/or PilH (He and Bauer, 2014), to stimulate TFP extension and retraction via the motor proteins PilB and PilT/PilU (Bertrand *et al*., 2010). Stimulation of the Chp system simultaneously regulates CyaB activity (Fulcher *et al*., 2010; Inclan *et al*., 2011), a membrane bound adenylate cyclase, that is the primary source of the second messenger 3′, 5′-cyclic monophosphate (cAMP) (Wolfgang *et al*., 2003). cAMP binds to the transcriptional regulator Vfr to modulate transcription of >200 genes, including key virulence factors such as the type II and type III secretion systems, quorum sensing and TFP (Wolfgang *et al*., 2003).

FimL mutants resemble ChpA and PilG mutants; null mutants of each exhibit wild type levels of intracellular pilin, decreased surface assembly of TFP, decreased twitching motility, decreased cAMP production and decreased T3SS expression (Whitchurch *et al*., 2004; Whitchurch *et al*., 2005; Fulcher *et al*., 2010; Inclan *et al*., 2011). However, the role of FimL remains unclear given that it is unlikely to undergo phosphorylation. We used a combination of affinity purification/mass spectrometry (AP-MS), immunoprecipitation and the bacterial two hybrid system (BACTH) to define a targeted protein–protein interaction network that links components of TFP and the Chp system to induce CyaB activity. We show that the Chp system accessory protein FimL directly interacts with FimV, a transmembrane component of the TFP assembly machinery and with PilG, one of the two response regulators associated with the histidine kinase ChpA. All three components are necessary for TFP-mediated activation of virulence circuits on surface attachment. Using fluorescent protein fusions, we show that FimL and PilG polar localization is dependent on FimV, while PilJ localizes independently of FimV. Investigation of a phosphorylation deficient PilG allele reveals that its phosphorylation plays a role in mechanochemical signaling but not in its polar localization or its ability to bind to FimL. We thus propose that FimL functions as a scaffold to spatially link TFP to the Chp chemosensory system to enable precise control of

cAMP-dependent upregulation of virulence genes on surface contact.

Results

AP-MS identifies interactions between FimL, FimV and PilG

To identify interacting partners of the Chp chemosensory system, we used AP-MS, adapting a protocol we recently applied to identification of pathogen-effector-host protein interactions (Mirrashidi *et al.*, 2015). We epitope tagged the Chp chemosensory signaling pathway output response regulator PilG (C-terminal HA) and the accessory protein FimL (C-terminal FLAG) and used allelic exchange to introduce each construct into its native chromosomal locus to ensure wild type levels of expression. Stab assays confirmed that twitching motility of the strains bearing the epitope-tagged protein were indistinguishable from wild type twitching motility (Supporting Information Fig. S1A), suggesting that the epitope tag does not interfere with protein function. Lysates were prepared from plate-grown bacteria, affinity purified over anti-HA or anti-FLAG beads and directly analyzed by mass spectrometry without gel purification. Each AP-MS was repeated at least four times, yielding at least four biological replicates. We used MiST and ComPASS algorithms to predict high confidence interactions between the baits and potential preys based on specificity, abundance and reproducibility (Sowa *et al.*, 2009; Verschueren *et al.*, 2015). From this analysis, we identified FimV and PilG as potential interacting partners of FimL (Fig. 1A, Supporting Information Table 1), based on their high MiST scores (0.81, top 0.8% for FimL and 0.66, top 9% for PilG) and ComPASS scores (179, top 1.7% score for FimL and 97, top 1.6% for PilG).

FimL directly interacts with FimV

To validate the FimL-FimV interaction, we performed co-immunoprecipitation experiments. A plasmid expressing an arabinose-inducible FimV-GFP fusion was introduced into PAO1 (PAO1 + pFimV-GFP) or PAO1 expressing FimL-FLAG at its native chromosomal locus (PAO1:: FimL-FL + pFimV-GFP). Lysates prepared from plate-grown arabinose-induced bacteria were immunoprecipitated using anti-FLAG coated beads and immunoblotted with antibodies to GFP or to FLAG. FimV-GFP co-immunoprecipitated with FimL-FLAG (PAO1:FimL-FL + pFimV-GFP) but not with untagged FimL (PAO1 + pFimV-GFP) (Fig. 1B). We attempted to immunoprecipitate with anti-GFP beads without success. In control experiments, neither FimL-FLAG nor FimV-GFP were immunoprecipitated from strains lacking pFimV-GFP (PAO1 or PAO1:FimL-FL; Fig. 1B).

A

Bait	Prey	MiST	ComPASS
FimL	FimV	0.81	179
PilG	FimL	0.66	97
PilG	FimV	0.63	30

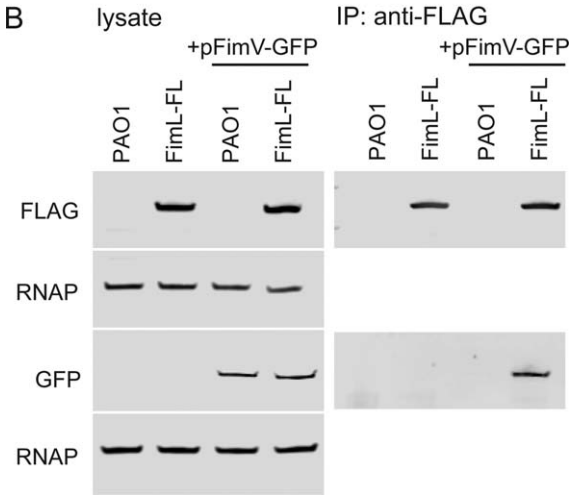

Fig. 1. FimL interacts with FimV.
A. MiST and ComPASS scores of selected preys of interest identified for FimL-FLAG and PilG-HA by AP-MS.
B. FimV-GFP co-immunoprecipitates with FimL-FLAG. PAO1 or PAO1 expressing FimL-FLAG from the chromosomal locus (FimL-FL) were transformed with a plasmid expressing FimV-GFP (pFimV-GFP). Untransformed strains serve as controls. Lysates (Left panel) and immunoprecipitations with anti-FLAG beads (right panel) were immunoblotted with the indicated antibodies. RNA polymerase (RNAP) serves as a loading control. The immunoblots shown are representative of three experiments.

While these studies confirm that FimL interacts with FimV in *P. aeruginosa*, we employed the BACTH assay (Karimova *et al.*, 1998; Battesti and Bouveret, 2012) to determine whether this interaction was direct. In this assay, the bait and prey are co-expressed in an *E. coli* adenylate cyclase mutant as fusions with one of two fragments (T18 or T25) from the catalytic domain of the *Bordetella pertussis* adenylate cyclase. Interaction of the two hybrid proteins results in functional complementation of adenylate cyclase activity, with resultant cAMP synthesis and transcriptional activation of β-galactosidase. The output can be detected by colony color on indicator agar plates or by quantitative measurement of β-galactosidase activity in liquid-grown cultures. BACTH is particularly useful for studying interactions between membrane proteins as well as cytosolic proteins (Karimova *et al.*, 2005). It has been successfully applied to studying the interactions

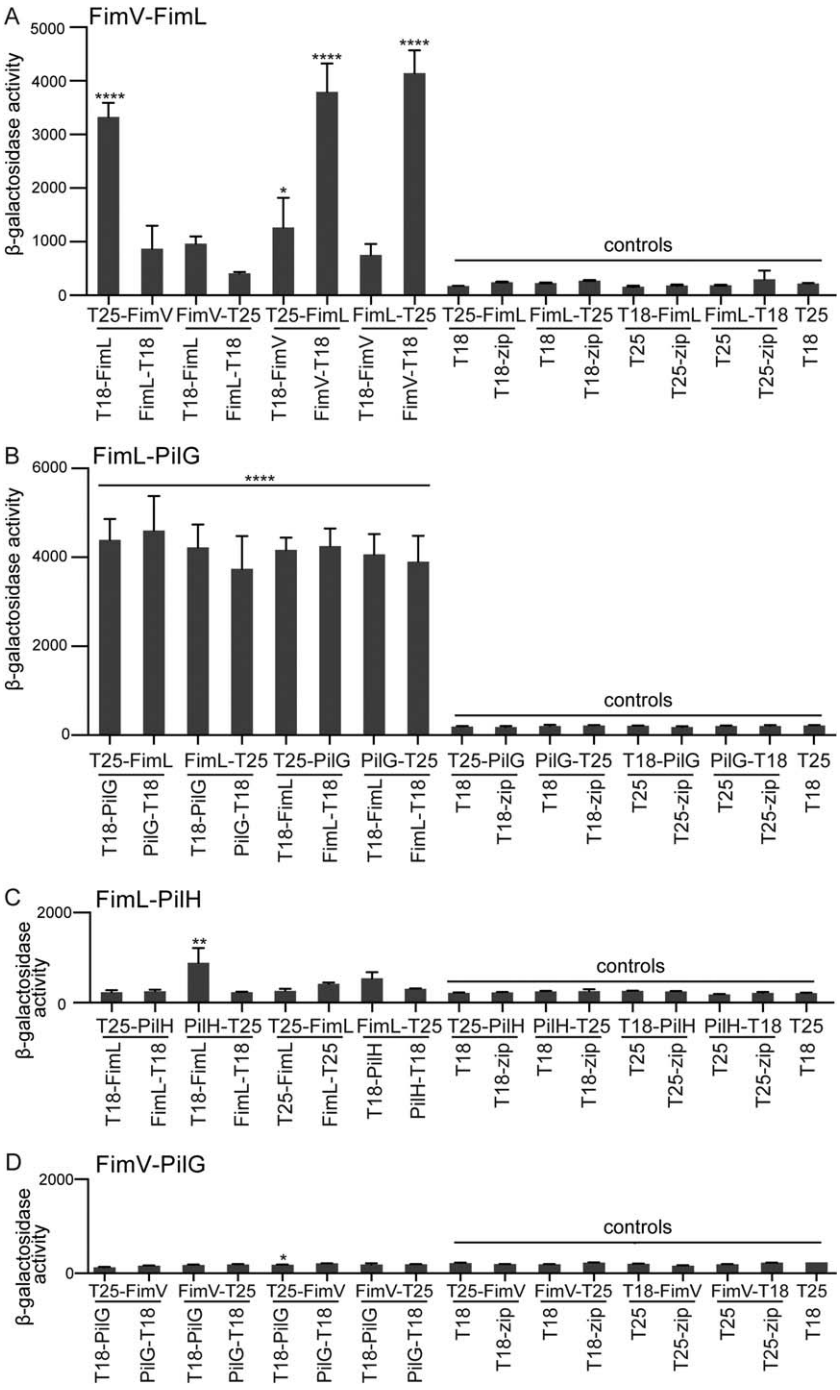

Fig. 2. FimL interacts directly with FimV and PilG by BACTH. β-galactosidase assays were performed on liquid-grown BTH101 *E. coli* transformed with the indicated plasmid pairs. Results are expressed as Miller units of β-galactosidase activity (A_{420} min^{-1} mL^{-1} of cells measured at OD_{600}). Shown are Mean ± SEM ($N = 3$ biological replicates with three technical replicates).
A. ****$P \leq 0.0001$ for T25-FimV/T18-FimL, T25-FimL/FimV-T18, FimL-T25/FimV-T18 and $P \leq 0.05$ for T25-FimL/T18-FimV plasmid pairs relative to all controls.
B. ****$P \leq 0.0001$ for all combinations of FimL and PilG relative to all controls.
C. **$P \leq 0.01$ for PilH-T25/T18-FimL relative to all controls.
D. *$P \leq 0.05$ for T25-FimV/T18-PilG relative to some controls (FimV-T25/T18-zip, T18-FimV/T25 and T25/T18).

between *Neisseria meningiditis* TFP proteins (Georgiadou *et al*., 2012).

We fused FimV and FimL to the N- or C-terminus of T18 or T25 to generate all eight possible combinations. Plate grown bacteria were visually inspected for colony color on MacConkey plates followed by quantitative β-galactosidase assays of liquid-grown bacteria (Fig. 2A). In some experiments, we quantified the signal generated by the interaction between two domains of a leucine zipper (T25-zip + T18-zip) as a positive control (see Fig. 6B). For negative controls, we assayed *E. coli* co-transformed with the T18 and T25 plasmids without inserts or with a single candidate fusion protein co-transformed with a plasmid expressing only the reciprocal T18 or T25 fragment or fused to a control zip protein domain (Fig. 2A).

All controls gave the expected results (Fig. 2A). Of the eight possible FimL-FimV combinations, robust and statistically significant positive interactions were detected for four pairs (Fig. 2A; T25-FimV/T18-FimL; T25-FimL/T18-FimV; T25-FimL/FimV-T18; and FimL-T25/FimV-T18). Although other combinations of FimV and FimL fused to the T18 and T25 domains might have been predicted to reconstitute adenylate cyclase activity, it is not unusual that only a subset of combinations yield positive interactions (Battesti and Bouveret, 2012). Nonetheless, the combination of AP-MS, directed co-immunoprecipitations in *P. aeruginosa*, and the BACTH assays demonstrate that FimL can directly interact with FimV.

PilG directly interacts with FimL but not with FimV

Guided by our AP-MS results, we tested whether PilG directly interacts with FimL and/or with FimV using the BACTH system (Fig. 2B and D). As a negative control, we also assayed the interaction between FimL and PilH (Fig. 2C). These two Chp system output response regulators PilG and PilH share 32% amino acid identity but have distinct phenotypes. Loss of PilG function results in decreased surface levels of TFP and cAMP levels, whereas loss of PilH function leads to increased surface levels of TFP and cAMP levels (Bertrand, 2010; Fulcher *et al.*, 2010). The BACTH assay indicated that all eight combinations of FimL and PilG interacted (Fig. 2B), with an approximately 20-fold increase over controls ($P \leq 0.0001$). In contrast, seven out of eight FimL-PilH combinations demonstrated no statistically significant increase in β-galactosidase activity, and only a small increase was observed for the PilH-T25/T18-FimL interaction (approximately 3.5-fold over controls ($P \leq 0.01$). Finally, we were unable to detect any interactions between PilG and FimV by BACTH (Fig. 2D). Together, these results suggest that FimL directly interacts with PilG but not with the closely related protein PilH. As PilG does not directly bind to FimV, their observed interaction in the AP-MS data set likely reflects their shared direct binding with FimL.

FimV is epistatic to FimL. FimV and FimL mutants have similar defects in cAMP production but can be distinguished by differences in twitching motility (Fulcher *et al.*, 2010). PAO1Δ*fimL* has reduced twitching motility when assayed by the standard subsurface stab assay, whereas the twitching motility defect in PAO1Δ*fimV* is more severe, similar to that of a mutant which lacks TFP altogether, PAO1Δ*pilA* (Wehbi *et al.*, 2011) (Fig. 3A). These observations are consistent with the notion that FimV functions in a required mechanical role for

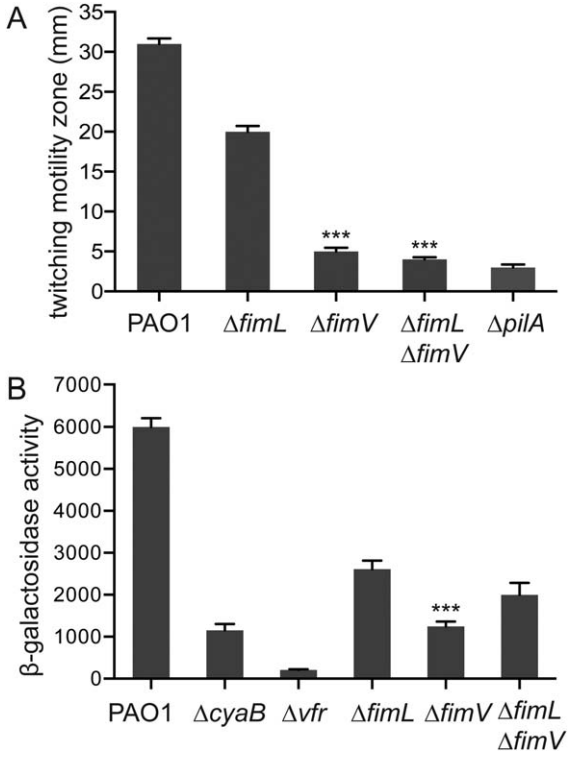

Fig. 3. FimV is epistatic to FimL.
A. Subsurface stab assays of the indicated strains. Shown are mean ± SEM ($N = 5$) of the twitching zone diameter measured at 24 h after inoculation. *** $P \leq 0.0001$ compared to PAO1Δ*fimL*.
B. β-galactosidase activity (A_{420} min^{-1} mL^{-1} of cells measured at OD_{600}) of the indicated strains expressing the *lacp*$_1$-*lacZ* reporter gene. cAMP levels directly correlate with β-galactosidase activity from the *lacp*$_1$ promoter. Shown are mean ± SEM ($N = 5$).
*** $P \leq 0.001$ PAO1Δ*fimL* compared to PAO1Δ*fimV*.

TFP assembly whereas FimL functions in a regulatory manner. We predicted that the double mutant, Δ*fimL*Δ*fimV*, should have the same phenotype as the Δ*fimV* mutant. We, therefore, constructed a Δ*fimL*Δ*fimV* double mutant strain bearing a β-galactosidase transcriptional reporter gene under control of the *E. coli lacp1* cAMP-dependent promoter (Fulcher *et al.*, 2010) integrated into the CTX phage attachment site on the chromosome. Twitching motility was quantified by subsurface stab assay and cAMP activity assayed by cAMP-dependent reporter gene (β-galactosidase) activity. The twitching motility of PAO1Δ*fimL* was intermediate to that of PAO1, PAO1Δ*fimV* and PAO1Δ*pilA*, whereas the twitching motility of PAO1Δ*fimL*Δ*fimV* resembled that of PAO1*fimV* (Fig. 3A). Thus, *fimV* is genetically epistatic to *fimL* for twitching motility. The results with the cAMP-dependent β-galactosidase assays were not as clear (Fig. 3B). As expected, PAO1Δ*vfr* had nearly undetectable β-galactosidase activity, since the cAMP-dependent reporter absolutely requires Vfr, whereas the Δ*cyaB* and Δ*fimV* mutants

had low but detectable β-galactosidase activity, consistent with the known role for CyaA in residual cAMP synthesis (Wolfgang *et al.*, 2003). β-galactosidase activity in PAO1Δ*fimL* was approximately twofold higher compared to Δ*fimV* ($P \leq 0.001$), whereas the double mutant, PAO1Δ*fimL*Δ*fimV*, had β-galactosidase levels intermediate to PAO1Δ*fimL* and PAO1Δ*fimV*. These differences did not reach statistical significance.

FimL, FimV and PilG are essential for surface contact-mediated activation of the cAMP/Vfr-dependent virulence pathways. We recently showed that TFP function as mechanosensors that regulate surface-induced gene expression through the Chp system-cAMP/Vfr, and require PilA, PilJ, ChpA, CyaB and Vfr (Persat *et al.*, 2015a). We quantified surface-dependent activation of a fluorescent transcriptional reporter gene, *PaQa-YFP*, compared to a constitutively expressed mKate reporter (*pRpoD-mKate*) at the single cell level to determine whether FimL, FimV or PilG actively participate in this pathway. We utilized the *PaQa*-YFP reporter as it is highly induced on transition from liquid growth to growth on a solid surface and has been shown to be regulated by the cAMP/Vfr system (Persat *et al.*, 2015a). Moreover, the fluorescence readout provides a very sensitive means of quantifying surface-mediated activation over very short times scales and at the single cell level. In PAO1, *PaQa-YFP* expression was enhanced threefold when grown on a solid agar surface compared to growth in the same media in liquid, whereas expression of the reporter gene was not increased in Δ*fimL*, Δ*fimV*, Δ*fimL*Δ*fimV* or in Δ*pilG* mutants during growth on solid media compared to growth in liquid media (Fig. 4). We conclude that FimL, FimV and PilG are essential for surface-contact mediated activation of the cAMP/Vfr transcriptional pathway.

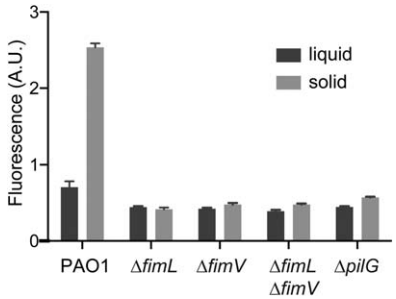

Fig. 4. FimL, FimV and PilG are required for TFP-dependent surface sensing. Contact-dependent cAMP/Vfr-dependent gene transcription was quantified using the *PaQa* reporter fused to YFP. PrpoD-mKate, a constitutive promoter fusion, served as an internal control. PAO1 grown on agarose hydrogels for 4 h display higher PaQa-YFP/PrpoD-mKate fluorescence ratio (arbitrary units) compared to liquid grown cells. In contrast, the PaQa-YFP/PrpoD-mKate fluorescence ratio PAO1Δ*fimL*, PAO1Δ*fimV*, PAO1Δ*fimLfimV* and PAO1Δ*pilG* mutants was not increased in solid compared to surface growth. The individual fluorescent ratios of ~ 100 cells were determined. Shown is the mean ± SEM of 3–4 biological replicates.

FimL and PilG localization depend on FimV. In addition to the TFP structural proteins, some regulatory components of the TFP as well as components of the Chp and cAMP/Vfr pathway are polarly localized, including PilB, PilT, FimL and CyaB (Chiang *et al.*, 2005; Inclan *et al.*, 2011). Based on our interaction results, we hypothesized that FimL or FimV may help co-localize components of TFP and Chp system. We thus tested whether FimL, PilG or PilJ localization was dependent on FimV, FimL, ChpA or PilG. FimL-GFP was introduced into the chromosomal locus by allelic exchange in the wild type or appropriate mutant backgrounds, whereas PilJ-GFP and PilG-GFP were expressed from a plasmid and transformed into informative mutant backgrounds. PAO1 expressing FimL-GFP exhibited wild type twitching motility, indicating that the fusion protein was functional (Supporting Information Fig. S1C). Plasmid-expressed PilJ-GFP and PilG-GFP showed partial complementation of twitching motility (Supporting Information Fig. S1B). Remarkably, FimL-GFP and PilG-GFP lost bipolar localization and appeared cytosolic in PAO1Δ*fimV* but retained polar localization in PAO1Δ*chpA* (Fig. 5A and C), indicating that the polar localization of FimL and of PilG is not an artifact of fusion to GFP. FimL-GFP retained its polar localization in PAO1Δ*pilG* (Fig. 5A). PilG-GFP retained polar localization in PAO1Δ*fimL*, suggesting that PilG may also localize through interaction with a redundant, FimV-dependent process or ChpA. Of note, PilJ-GFP polar localization was independent of ChpA, FimV and PilG (Fig. 5G). Western blot analysis demonstrated that the levels of FimL-GFP, PilG-GFP and PilJ-GFP were minimally changed in the mutant backgrounds (Fig. 5B,D,H), eliminating the possibility that the altered localization of FimL-GFP or PilG-GFP was a function of instability of the fusion protein. We thus conclude that *P. aeruginosa* utilizes at least two nonredundant mechanisms by which the Chp components are localized to the pole. FimL and PilG polar localization is primarily dependent on FimV, whereas the mechanism by which PilJ is restricted to the poles is distinct and remains to be elucidated.

PilG phosphorylation mediates contact-dependent cAMP production but not interaction with FimL. Our results thus far suggest that FimV/FimL/PilG association plays a central role in the TFP-Chp-CyaB mechanochemical signaling regulating cAMP production and Vfr-dependent transcription. To determine whether the interactions between these three proteins is dependent upon signaling events, we assessed the phenotypes of a Δ*pilG* mutant in which the putative phosphoacceptor aspartate

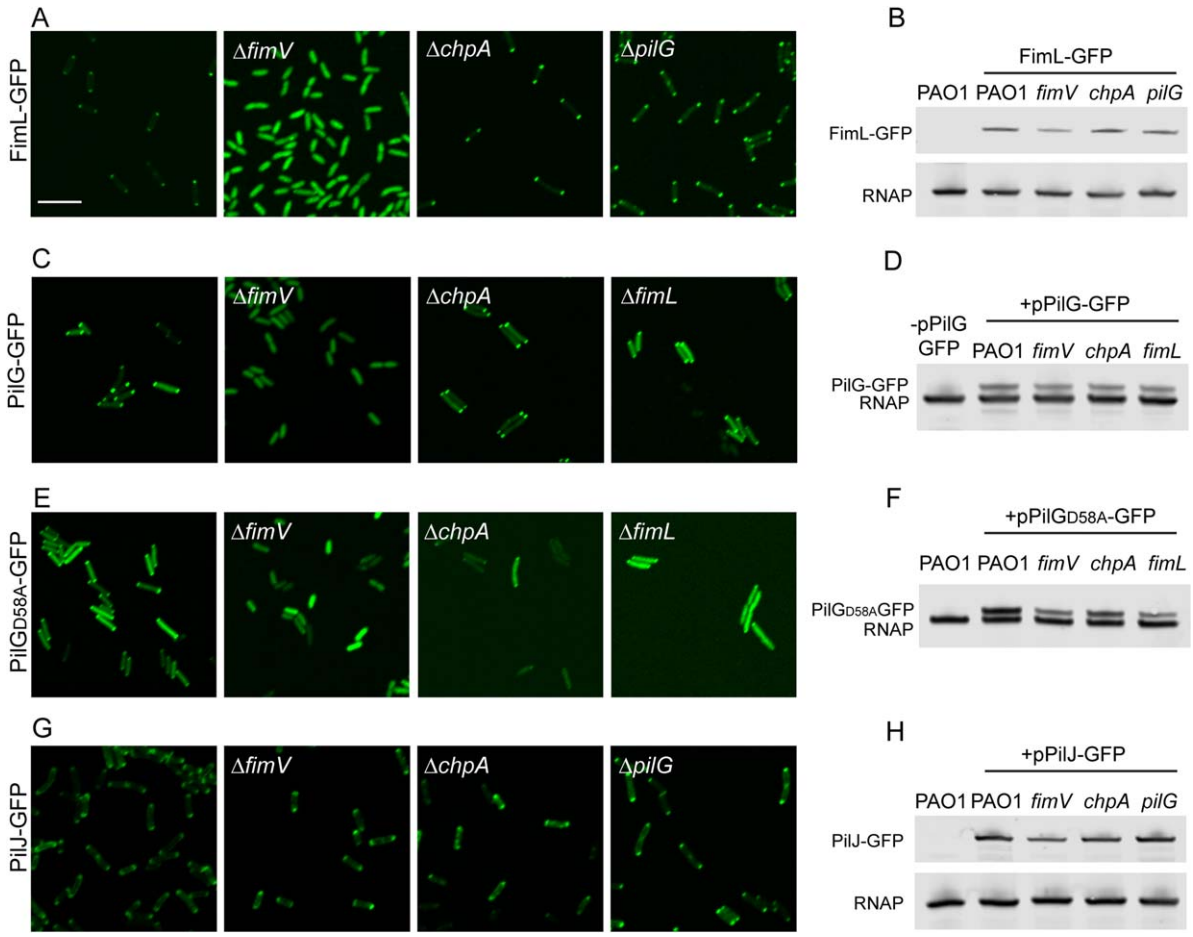

Fig. 5. Subcellular localization of FimL-GFP, PilJ-GFP and PilG-GFP. The indicated PAO1 strains expressing (A) FimL-GFP from the chromosome, (C) plasmid-encoded PilG-GFP (pPilG-GFP), (E) plasmid-encoded $PilG_{D58A}$-GFP ($pPilG_{D58A}$-GFP) or (G) plasmid-encoded PilJ-GFP (pPilJ-GFP) in wild-type PAO1, PAO1Δ*fimV*, PAO1Δ*chpA* and PAO1Δ*fimL* mutants were grown on agar pads with 0.02% arabinose induction for 4 h and then examined by confocal microscopy. Scale bar represents 5 μm. (B,D,F,H) Immunoblot of lysates prepared from the indicated strains probed with the anti-GFP (top band) or anti-RNAP, a loading control (bottom band).

residue was replaced with alanine ($PilG_{D58A}$) (Bertrand *et al.*, 2010). The phenotype of $pilG_{D58A}$ resembles that of a Δ*pilG* mutant for twitching motility (Bertrand *et al.*, 2010), cAMP production (Fig. 6A), and surface-dependent gene expression (Fig. 6B). Surprisingly, the phosphorylation deficient mutant is still able to bind to FimL as assessed by BACTH (Fig. 6C) and to localize to the poles in a FimV-dependent but ChpA-independent manner (Fig. 5E). Although there is substantial cytoplasmic GFP signal, polar puncta are still visible in the Δ*chpA* or Δ*fimL* mutant, in contrast to the Δ*fimV* mutant. No interaction between $PilG_{D58A}$ and FimV could be detected by BACTH. Thus, we conclude that FimL-PilG phosphorylation is not required for binding to FimL or for its polar localization but that it is required for the mechanochemical signaling. This result is consistent with our model that FimL functions as a scaffold protein in colocalizing PilG to FimV at the cells poles, thus promoting their interaction.

FimL and FimV are conserved in gamma-proteobacteria encoding TFP and a Chp-like chemosensory signaling system

Chemotaxis-like regulatory systems have been co-opted to regulate diverse behaviors in bacteria (He and Bauer, 2014), and Chp-like chemosensory systems have been identified in other bacteria (Whitchurch *et al.*, 2004). We performed phylogenetic analyses to determine whether other TFP-expressing bacteria encode FimL, FimV, Chp system and adenylate cyclase homologs as a clue that they may have evolved mechanotransduction circuits using these modular components. We first searched the nonredundant protein database for bacteria with complete genome sequences to identify a subset encoding TFP (Fig. 7, shaded orange) to which we manually included additional TFP-encoding medically relevant and well characterized organisms (Fig. 7, shaded gray). Among these organisms, we then looked for homologs of the

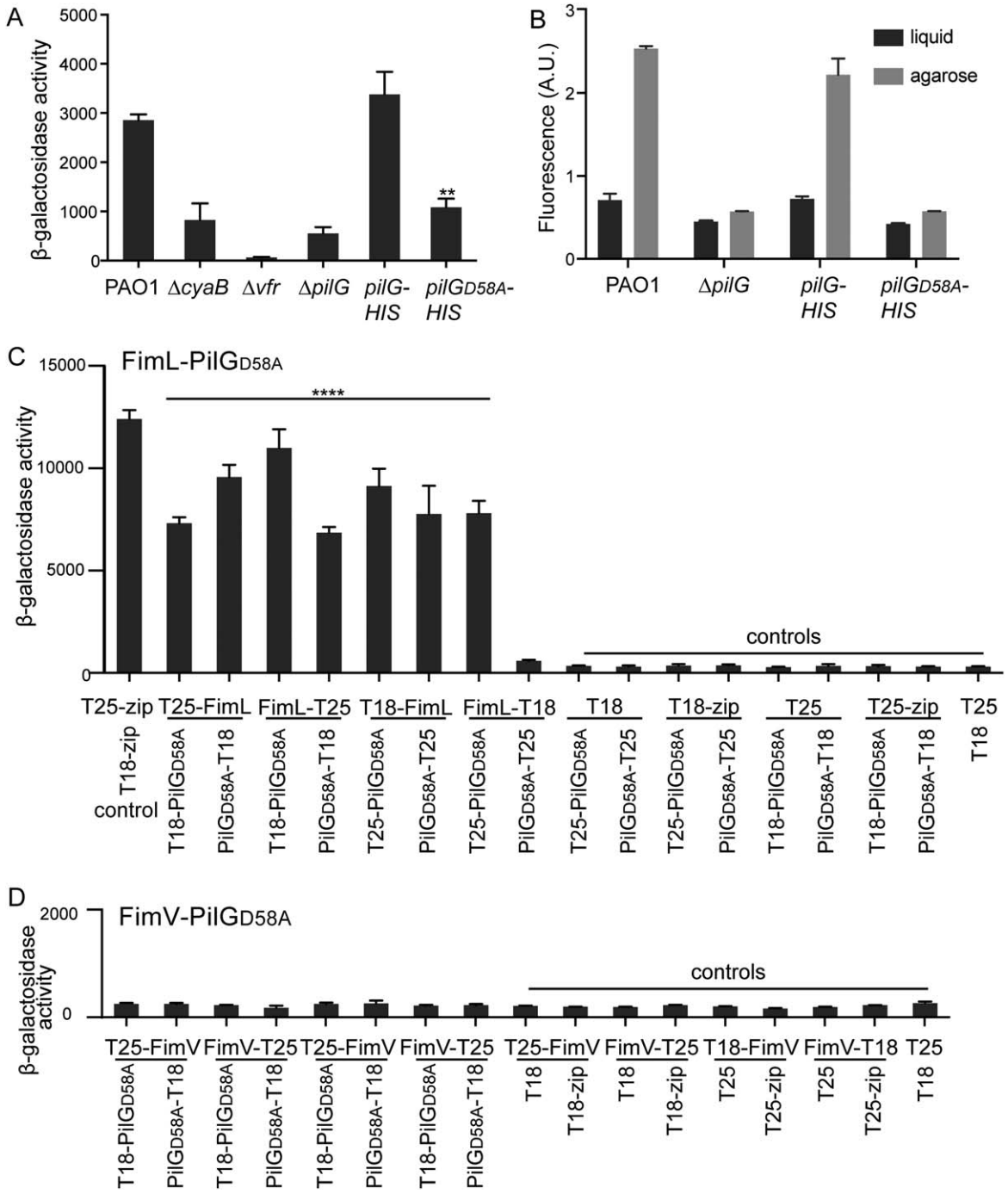

Fig. 6. PilG phosphorylation is required for cAMP production and contact-dependent gene activation but not for its association with FimL or its FimV-dependent polar localization.

A. β-galactosidase activity (A_{420} min^{-1} mL^{-1} of cells measured at OD_{600}) of the indicated strains expressing the P*lacp*$_1$-*lacZ* reporter gene. cAMP levels directly correlate with β-galactosidase activity from the *lacp*$_1$ promoter. Shown are mean ± SEM ($N = 2$ biological replicates, with three technical replicates each). ** $P \leq 0.005$ PAO1::$PilG_{D58A}$-HIS compared to PAO1::PilG-HIS. The difference between PAO1 compared to PAO1::PilG-HIS was not significant.

B. Contact-dependent cAMP/Vfr-dependent gene transcription was quantified as described for Fig. 4. The individual fluorescent ratios of ~ 100 cells were determined. Shown is the mean ± SEM of 3–4 biological replicates.

C and D. β-galactosidase assays were performed on liquid-grown BTH101 *E. coli* transformed with the indicated plasmid pairs. Results are expressed as Miller units of β-galactosidase activity (A_{420} min^{-1} mL^{-1} of cells measured at OD_{600}). Shown are Mean ± SEM ($N = 3$ biological replicates with three technical replicates each). C. **** $P \leq 0.0001$ for all combinations of FimL/$PilG_{D58A}$ pairs relative to all negative controls except FimL-T18/$PilG_{D58A}$-T25, D. ns for all combinations of FimV/$PilG_{D58A}$ relative to all controls.

Chp system, FimV, FimL and CyaB. We identified several bacteria encoding predicted homologs of the TFP assembly proteins and Chp-like chemosensory systems (Fig. 7). Many species that encode both TFP and Chp chemosensory system homologs also encode predicted FimV, FimL and CyaB homologs. In *Vibrio* and *Acinetobacter* species, we identified FimV homologs with variations on the PAO1 FimV architecture, which contains an N-terminal peptidoglycan binding domain (LysM domain) and a C-terminal FimV-domain. *Vibrio cholera* and *V. vulnificans* encoded longer FimV proteins, 1620 and 1951 aa, respectively compared to 919 aa in PAO1. The N- and C-terminal domains of *Acinetobacter* sp. FimV were split, i.e. were encoded in two adjacent open reading frames. The upstream gene encodes a LysM domain and the downstream gene encodes motifs of acidic-residue containing low complexity repeats and a conserved domain annotated as FimV_Cterm in the NCBI conserved domain database. These features are common in other FimV homologs. For *Vibrio* and *Acinetobacter*, more than one species was investigated to rule out potential genome sequencing errors. Together, this analysis suggests that diverse bacteria may have evolved a common strategy for mechanochemical signal transduction that regulates cAMP-dependent gene transcription, although the outputs of such system remain to be determined in each species.

Discussion

Mechanics have only been recently recognized as an important modulator of bacterial physiology (Belas, 2014; Persat *et al.*, 2015b), and the specific interactions mediating transduction of mechanical input into a biochemical output in bacteria are yet to be explored. In *P. aeruginosa*, TFP retraction on binding to a solid surface serves as a mechanical signal to activate the Chp chemosensory-like system to increase CyaB-dependent cAMP production and upregulate cAMP/Vfr-dependent virulence gene expression (Persat *et al.*, 2015a). We have made the unexpected discovery that FimL, a protein whose function has remained elusive, may function as a scaffold to link FimV – a peptidoglycan binding protein that couples the inner and outer membrane components of TFP – with PilG, one of the two CheY-like response regulators associated with the Chp system (Fig. 8). Using multidisciplinary approaches, including AP-MS, co-immunoprecipitations, subcellular localization and BACTH, we provide evidence that FimL binds directly to FimV and to PilG. We further show that FimV is required for polar localization of FimL and PilG. While PilG phosphorylation is required for signaling through the TFP-Chp-CyaB pathway, its phosphorylation is not required for the FimV-FimL-PilG interactions, consistent with a model where FimL plays the role of a scaffold protein. Our phylogenetic analysis suggests that linkage of these pathways may occur in other environmental

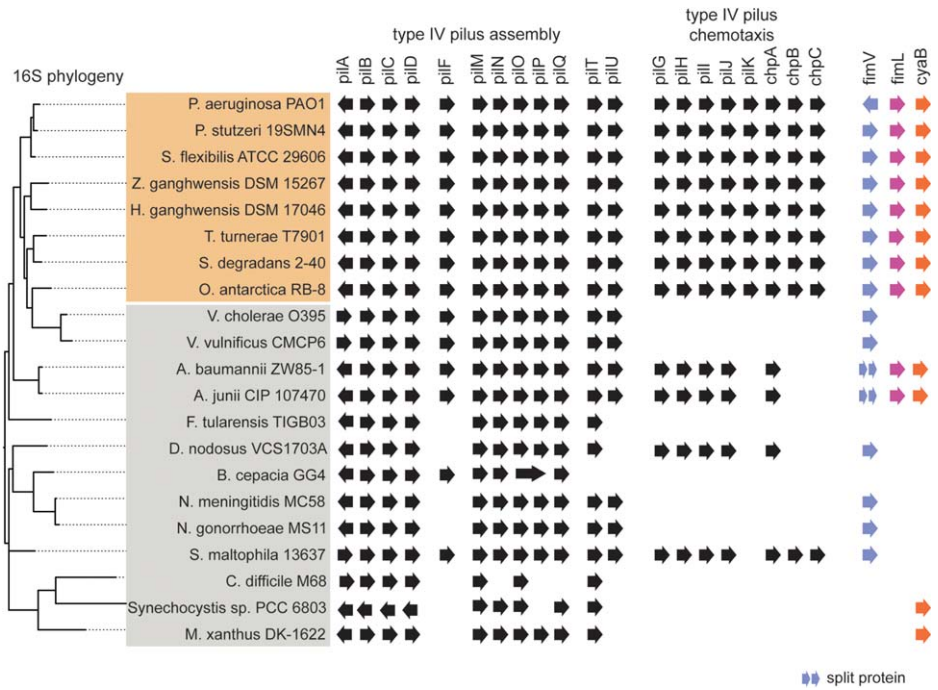

Fig. 7. Phylogenetic analysis of TFP, Chp system and accessory genes in select bacterial species. Bacterial species selected for high TFP assembly homology (shaded in orange) and species selected for medical relevance (shaded in gray) are listed left. The presence of all genes was determined by tblastn of PAO1 proteins against the whole genome sequence of the respective bacterial strain and analyzed by HHPred and blastp analysis. Gene orientation is indicated. Bacterial species were clustered by full-length 16S phylogeny.

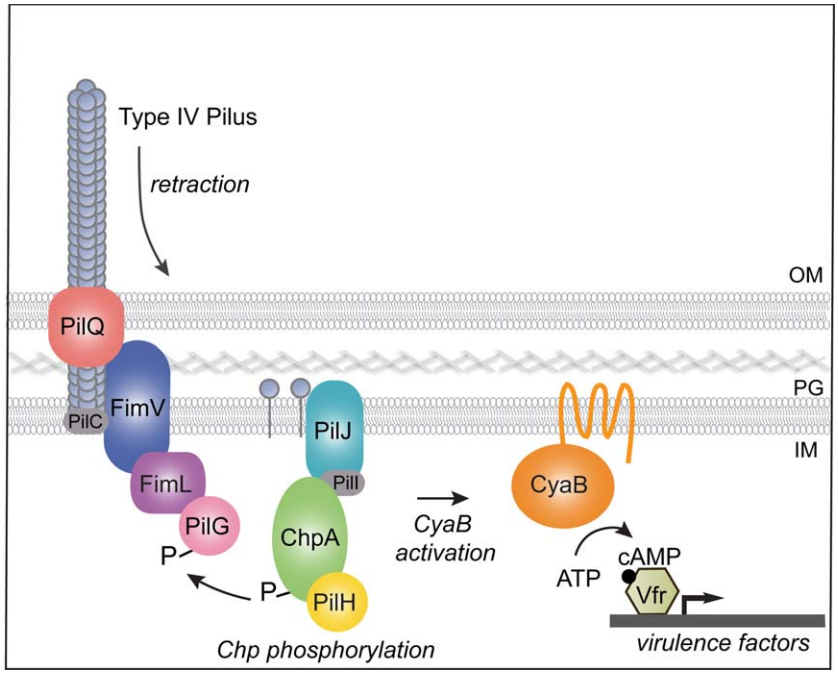

Fig. 8. Model for surface-activated regulation of cAMP/Vfr-dependent virulence factors. On surface binding, TFP retracts. Depolymerized or conformationally altered pilin monomer binds to PilJ in the periplasmic and/or inner membrane space, which leads to ChpA histidine kinase autophosphorylation. A phosphoryl group is subsequently transferred to the response regulator PilG, which leads to stimulation of the membrane bound adenylate cyclase CyaB, cAMP production and activation of cAMP/Vfr-dependent virulence circuits. FimV is required for polar localization of FimL and PilG. Our studies show that FimV, FimL and phosphorylation-competent PilG are required to stimulate cAMP production and surface-mediated activation of a cAMP/Vfr-dependent promoter. In addition, we show that FimL binds to FimV and to PilG, although whether they form a trimolecular complex is unknown. We speculate that localization of PilG to the pole through its binding to FimL and FimV increases its local concentration and facilitates its phosphorylation by ChpA.

organisms including important human pathogens, such as *A. baumannii, V. cholera and V. vulnificans*. Thus, signaling in response to surface contact may represent a widespread strategy that allows bacteria to rapidly sense changing mechanical environments, both in the environment and during human infections.

Our approach to screen for interactions between components of complex chemosensory systems can be applied in a high throughput fashion to comprehensively establish PPI networks in bacteria and to complement other approaches, such as global BACTH (Battesti and Bouveret, 2012), yeast two hybrid screens (Fields and Song, 1989), and chemical cross-linking mass spectrometry (Herzog *et al.*, 2012). Surprisingly, their application to *P. aeruginosa* has been somewhat limited thus far (Navare *et al.*, 2015). For our studies, we epitope-tagged the chromosomal gene of interest. By directly applying the affinity-purified eluate to mass spectrometry, we eliminated the need to visualize bands by gel chromatography, allowing us to potentially identify low affinity and/or transient interactions. The AP-MS strategy is also likely highly specific: we identified an interaction between PilG and FimL, but not between the closely related protein PilH and FimL, and we confirmed the specificity by BACTH.

Our work suggests that FimL functions as a scaffold linking FimV and PilG at the pole, where TFP, the Chp chemosensory system and the CyaB adenylate cyclase may interact. Although FimL is highly homologous to the N-terminus of ChpA including the two most N-terminal Hpt domains, the phospho-accepting conserved histidine residues have been replaced by glutamines in all species examined. Thus, it is unlikely that FimL directly participates in the ChpA phosphorelay circuit. While the interactions between response regulators and their binding partners is often too transient to be captured by traditional biochemical assays, we observed a robust interaction between FimL and PilG by BACTH. BACTH represents a more sensitive detection platform due to overexpression of the putative interacting proteins. Alternatively, the interaction between PilG and FimL may be distinct from the canonical interaction between a response regulator and its cognate histidine kinase or its downstream target, a model that we favor. The PilG:FimL interaction is also highly specific, and, while the distinct domains and residues of PilG and FimL that mediate their interaction await experimental verification, it is intriguing that PilG encodes short N- and C-terminal extensions absent in PilH.

Robust connection of the TFP coupling complex, comprising PilMNOP, to the peptidoglycan is thought to be the main function of FimV (Wehbi *et al.*, 2011). Our results now reveal an unexpected role for this protein: by interacting with FimL, FimV couples TFP activity with Chp signaling through PilG. The C-terminus of FimV encodes multiple TPR repeats which are annotated as protein binding sites (Wehbi *et al.*, 2011) and may be the site of FimL interaction. This model is consistent with reports of FimV homologs in *Vibrio* and *Shewanella* species that function as polar hubs to recruit, through acidic repeat motifs found in the C-terminus, client proteins such as chemotaxis arrays and proteins involved in chromosome segregation (Yamaichi *et al.*, 2012, Rossmann *et al.*, 2015). We hypothesize that the FimV-

FimL-PilG interactions could serve to (i) localize PilG close to its cognate histidine kinase (ChpA) and to the TFP, thus increasing the local concentration of PilG and increasing the probability of phosphorylation in response to tensile forces in TFP (ii) link an active form of PilG to CyaB to activate synthesis of cAMP or (iii) sequester the response regulator PilG from its cognate histidine kinase, ChpA. Future experiments will be directed to distinguish between these models.

We propose the following model of early events following TFP adhesion to a solid surface, which integrates several published studies (Whitchurch *et al.*, 2005; Leech and Mattick, 2006; Bertrand *et al.*, 2010; Fulcher *et al.*, 2010; Inclan *et al.*, 2011; Persat *et al.*, 2015a) (Fig. 8). On contact with a solid surface, TFP experience tension on retraction, which may lead to conformational changes in the pilin subunit (Beaussart *et al.*, 2014). This event leads to modulation of the interaction between PilA and the periplasmic domain of PilJ, the MCP receptor of the Chp chemosensory system, leading to increased ChpA autophosphorylation on one or more of its Hpt domains. The phosphoryl group is subsequently transferred to response regulator PilG, though the route of phosphotransfer remains incompletely defined. Phosphorylated PilG appears to have two outputs: stimulation of TFP extension and retraction *via* PilB and PilT/PilU, and activation of the membrane bound adenylate cyclase, CyaB. At later stages, other signaling systems interact with the Chp system (Almblad *et al.*, 2015; Luo *et al.*, 2015). Activation of cAMP/Vfr-dependent gene expression, together with another two component system FimS/AlgR, upregulates expression of PilY1, a TFP accessory component. Cell surface-associated PilY1 signals through the TFP alignment complex (PilMNOPQ) and the diguanylate cyclase SadC to activate production of cyclic di-GMP, which in turn downregulates cAMP production through an unidentified mechanism (Almblad *et al.*, 2015; Luo *et al.*, 2015). Together, the successive activation of cAMP and cyclic di-GMP allows *P. aeruginosa* to first activate virulence factors associated with acute infections (such as T3SS effectors) thus fending off predators as it transitions from a motile to sessile lifestyle, and then to deactivate this system while upregulating components such as exopolysaccharide to activate the biofilm developmental pathway and enhance resistance against antimicrobial compounds.

Our studies raise several questions regarding signal transduction between TFP, the Chp system and CyaB. First, does FimL contact FimV and PilG simultaneously, or are these mutually exclusive interactions? It is intriguing that mutants either lacking FimL or overexpressing FimL have similar phenotypes, including loss of surface pili, decreased twitching motility and decreased cAMP levels (Inclan *et al.*, 2011). This result suggests that the stoichiometry of FimL relative to FimV and/or PilG is an important aspect of the signaling cascade. Second, why is PilG mislocalized in a Δ*fimV* mutant but not in a Δ*fimL* mutant? Perhaps PilG interacts with another protein at the cell pole which is linked to FimV. Third, could perturbations in peptidoglycan affect the ability of FimV to bind to FimL, and is this important in the ability of the TFP to serve as a surface-activated mechanosensor? Finally, is the association of FimV-FimL-PilG required for mechanochemical signaling?

The planktonic lifestyle has been conventionally associated with acute infections while the sessile, biofilm-associated state is associated with chronic, highly antibiotic resistant infections (Tolker-Nielsen, 2014). Recent work from our lab and others has begun to challenge this paradigm, as many 'acute' human *P. aeruginosa* infections likely involve biofilms (Hall-Stoodley and Stoodley, 2009; Hall-Stoodley *et al.*, 2012). Moreover, during the initial switch from the nonadherent planktonic growth phase to initial stages of biofilm formation, virulence factor circuits are activated by TFP-mediated contact (Persat *et al.*, 2015a). We posit that the initial contact-mediated upregulation of virulence factor circuits may be specifically beneficial to *P. aeruginosa* and may account for its ability to rapidly initiate infection on encountering a host at short timescales, before initiating a more persistent lifestyle. During the initial phases of biofilm formation, *P. aeruginosa* downregulates flagellar motility (Wolfgang *et al.*, 2003) and loses its ability to swim away and escape phagocytic predators. By rapidly inducing virulence factor circuits during transition to the sessile life style and early stages of biofilm formation, *P. aeruginosa* gains the ability to kill phagocytic predators, such as environmental amoeba or tissue neutrophils, and thus can overcome what would otherwise be a particularly vulnerable state before full biofilm development.

Experimental procedures

Bacterial strains and plasmids

Bacterial strains and plasmids used in this study are listed in Table 1. Bacteria were routinely inoculated from frozen glycerol stocks on Luria-Bertani (LB) 1.5% agar into liquid LB shaking with vigorous aeration at 250 r.p.m. at 37°C. *Escherichia coli* DH5α or competent stellar cells (Clontech) were used for amplifying plasmids. Plasmid DNA was introduced into PAO1 competent cells by electroporation or by conjugative mating with *E. coli* strain S17-1 to incorporate constructs into the chromosome for unmarked allelic exchange (Schweizer, 1992; West *et al.*, 1994; Hoang *et al.*, 2000). Antibiotic concentrations used for *E. coli*: tetracycline, 10 μg ml^{-1}; ampicillin, 100 μg ml^{-1}; carbenicillin, 50 μg ml^{-1}, gentamicin, 10 μg ml^{-1}, kanamycin 50 μg ml^{-1}; for *P. aeruginosa*: tetracycline, 100 μg ml^{-1}, carbenicillin, 250 μg ml^{-1}, gentamicin, 100 μg ml^{-1}.

PAO1Δ*fimV*, PAO1Δ*fimL*Δ*fimV*, all FimL-GFP strains, PAO1::FimL-FLAG and PAO1::PilG-HA and PAO1::PilH-HA were generated by standard allelic exchange protocols

(Whitchurch *et al.*, 2004). PAO1 was mated with S17-1 and pJB128 to construct PAO1::PilG-HA. pJB128 was constructed by subcloning *pilG-HA* from pJB142 as an SpeI fragment into pJB100 for PilG-HA. pJB142 was constructed by amplifying *pilG* from chromosomal PAO1 DNA using primers to generate an N-terminal XbaI site and a C-terminal HA-tag and HindIII site and cloning the pilG-HA fragment into pMBAD18G using XbaI/HindIII sites. PAO1Δ*fimV* and PAO1Δ*fimL*Δ*fimV* were constructed by mating S17-1 pJB100Δ*fimV* with PAO1 and PAO1Δ*fimL* respectively. pJB100Δ*fimV* was constructed by cloning the ΔfimV PCR product into SpeI sites of pJB100. The ΔfimV PCR insert was generated by amplifying 1000 bp upstream of *fimV*, 1000 bp downstream of *fimV* and then using overlap PCR to generate a fusion of these fragments with SpeI sites on the 5′ and 3′ ends and leaving the 7 codons of *fimV* to generate an in-frame chromosomal deletion. FimL-GFP strains were constructed by allelic exchange by mating S17-1 pYFI043 with PAO1, PAO1Δ*fimV*, PAO1Δ*chpA* and PAO1Δ*pilG* to generate PAO1::FimL-GFP, PAO1Δ*fimV*::FimL-GFP, PAO1Δ*chpA*::FimL-GFP and PAO1Δ*pilG*::FimL-GFP. pMBADFimV-GFP was generated by amplifying *fimV* from chromosomal PAO1 followed by cloning into the KpNI/XbaI sites of pMBAD18G-GFP. Bacterial two-hybrid (BACTH) constructs were generated by adding 15 nucleotides of homologous DNA to the desired insertion site of the BACTH vectors to primers used to amplify genes of interest from the PAO1 chromosomal DNA. The *P. aeruginosa* genes *fimL*, *pilG*, *pilH* and *fimV* were cloned into pKT25, pKNT25, pUT18 and pUT18C (Euromedex). The PCR products were ligated into linearized vectors using the BD In-fusion cloning kit (Clontech). The PilGD58A constructs were generated by using QuikChange Lightning (agilent) using the BACTH PilG vectors as templates. (Phusion polymerase and accompanying reagents (NEB) were used for all PCR protocols. Orientation and sequence of all plasmids was verified by sequencing. Fusion proteins were verified in *P. aeruginosa* strains via PCR and western blot analysis with anti-FLAG (Sigma), anti-HA (Sigma) or anti-GFP (Roche) antibodies. FimV deletion strains were verified by PCR. Primer sequences are available on request.

Affinity purification and Mass Spectrometry

LB cultures inoculated from a single colony were grown at 37° with vigorous aeration at 250 r.p.m. for 6 h. Hundred microliter of the culture was spread onto 1.5% LB plates or MinS plates (Nicas and Iglewski, 1984) containing appropriate antibiotics and grown overnight at 37°C. Bacteria were scraped from the plate and resuspended with vortexing and rapid pipetting in 5 ml PBS and OD_{600} was measured. Cell suspensions were diluted to $OD_{600} = 3$ in 2 ml PBS, centrifuged at 8000 *g*, the supernatants were discarded, and cell pellets were frozen. Pellets were resuspended in 2 ml lysis buffer (50 mM Tris-HCl, pH 7.5, 150 mM NaCl, 0.5% NP-40, 1 mg ml^{-1} lysozyme, protease inhibitor cocktail tablet [Roche], 25 U ml^{-1} benzonase [Invitrogen]). Lysates were incubated on ice for 20 min and sonicated (Branson sonicator 150) with a microtip for 10 s with 1 s manual pulsing (on setting 10, approximately 100 W), three times with minimum 1 min rest intervals on ice. Lysates were centrifuged for 20 min at 14,000 *g*, and the soluble portion was decanted and incubated with 50 μl beads as directed by the manufacturer. Beads were captured by low speed (1000 *g*) centrifugation or with a magnet, and the flowthrough was discarded. Bound beads were washed three times with 1 ml of wash buffer (50 mM Tris-HCl pH 7.5, 150 mM NaCl, 0.05% NP-40), vortexed briefly and centrifuged or captured with the magnet. Beads were washed additionally with buffer lacking NP-40 to remove detergent. Bound material was eluted from beads with 30 μl FLAG or HA peptide solution in TBS (100 ng/μl). Eluate were flash frozen in liquid nitrogen, thawed then trypsin digested for LC- MS/MS (Jager *et al.*, 2011, 2012). Digested peptide mixtures were analyzed on a Thermo Scientific Velos Pro ion trap MS system equipped with a Proxeon Easy nLC II high-pressure liquid chromatography and autosampler system. Each purification was performed at least four times. AP-MS samples were scored with MiST (Jager *et al.*, 2012) and ComPASS (Sowa *et al.*, 2009) algorithms. The algorithms are based on specificity, reproducibility and abundance of prey peptides identified and compared to mock controls and control tagged proteins. A MiST score of 0.81 represents the top 0.8% of MiST scores and the ComPASS score of 179 represents the top 1.7% of the scores for the FimL bait. MiST scores of 0.66 and 0.63 represent the top 9.0% and 9.6% respectively and a ComPASS score of 97 and 30 represent the top 1.6% and 4.6% of the scores for the PilG bait.

Co-immunoprecipitation in P. aeruginosa

Single colonies of PAO1, PAO1 + pFimV-GFP (pMBAD18G FimV-GFP), PAO1::FimL-FLAG, and PAO1::FimL-FLAG pMBAD18FGimV-GFP were inoculated into 2 ml LB cultures containing appropriate antibiotics. After 6 h growth at 37°C with vigorous aeration, 100 μl were plated onto LB plates and incubated overnight at 37°C in a humidified bag. All experiments performed using pFimV-GFP included gentamicin and 1% arabinose for plasmid selection and pFimV-GFP induction throughout all growth steps. Plates were scraped, resuspended in 5 ml of PBS and OD_{600} was measured. Cells were centrifuged at 8000 *g* for 10 min, washed with PBS and resuspended to $OD_{600} = 3$, centrifuged, and the pellet was frozen at −20°C. Frozen pellets were resuspended in 2 ml lysis buffer (50 mM Tris-HCl pH 7.5, 150 mM NaCl, 0.5% NP-40, 1 mg ml^{-1} lysozyme, 1 mM PMSF, benzonase). Lysates were processed as described for AP-MS. The beads were captured with the magnet and eluate was recovered, mixed with loading buffer and boiled for 5 min. Western blots were performed on all samples with 1:1000 dilution of anti-GFP antibody (Roche) and anti-RNAP antibody (Sigma) as a loading control. Co-IP and western blotting were performed three times and representative blots are shown.

Bacterial two-hybrid assay

BTH101 chemically competent cells were generated using the TSS protocol (Chung *et al.*, 1989) and co-transformed with 20 ng of each pK and pUT construct as described in the Euromedex manual. Cultures inoculated with single colonies were assayed for β-galactosidase activity as described (Battesti and Bouveret, 2012) using the 96-well

Table 1. Bacterial strains and plasmids.

Strain or plasmid	Genotype or relevant characteristic	Reference or source
E. coli strains		
DH5α	*fhuA2 lacΔU169 phoA glnV44 Φ80' lacZΔM15 gyrA96 recA1 relA1 endA1 thi-1 hsdR17*	Invitrogen
Stellar	*F–, endA1, supE44, thi-1, recA1, relA1, gyrA96, phoA, Φ80d lacZΔM15, Δ(lacZYA - argF) U169, Δ(mrr - hsdRMS - mcrBC), ΔmcrA, λ–*	Clontech
S17-1λ*pir*	*Thi pro hsdR recA RP4-2*(Tc::Mu)(Km::Tn7)	Simon *et al.* (1983)
BTH101	*F-, cya-99, araD139, galE15, galK16, rpsL1, hsdR2, mcrA1, mcrB1*	Euromedex, Karimova *et al.* (2001)
P. aeruginosa		
PAO1	Wild type	ATCC 15692 Holloway and Morgan (1986)
PAO1::FimL-FLAG	FimL-FLAG allelic exchange	Inclan *et al.* (2011)
PAO1Δ*fimV*	In-frame deletion of *fimV*	This study
PAO1::PilG-HIS	PilG-HIS allelic exchange	Bertrand (2010)
PAO1::$PilG_{D58A}$-HIS	$PilG_{D58A}$-HIS allelic exchange	Bertrand (2010)
PAO1Δ*fimL*Δ*fimV*	In-frame deletion of *fimL*, *fimV*	This study
PAO1Δ*pilA*	In-frame deletion of *pilA*	Bertrand *et al.* (2010)
PAO1Δ*cyaB*	In-frame deletion of *cyaB*	Inclan *et al.* (2011)
PAO1Δ*vfr*	In-frame deletion of *vfr*	Whitchurch *et al.* (2005)
PAO1Δ*pilG*	In-frame deletion of *pilG*	Bertrand *et al.* (2010)
PAO1Δ*chpA*	In-frame deletion of *chpA*	Bertrand *et al.* (2010)
PAO1::FimL-GFP	FimL-GFP allelic exchange	Inclan *et al.* (2011)
PAO1Δ*fimV*::FimL-GFP	In-frame deletion of *fimV*, FimL-GFP allelic exchange	This study
PAO1Δ*chpA*::FimL-GFP	In-frame deletion of *chpA*, FimL-GFP allelic exchange	This study
PAO1Δ*pilG*::FimL-GFP	In-frame deletion of *pilG*, FimL-GFP allelic exchange	This study
PAO1Δ*pilJ*	In-frame deletion of *pilJ*	Bertrand *et al.* (2010)
Plasmids		
pEX100T	Allelic exchange suicide plasmid, Ap^r, Cb^r	Tan *et al.* (1999)
pJB100	pEX100T derivative replacing SmaI site with the SpeI site	Bertrand *et al.* (2010)
pJB128	Allelic exchange construct, PilG-HA in pJB100, Ap^r, Cb^r	Jacob Bertrand
pJB125	Allelic exchange construct, PilH-HA in pEX100T, Ap^r, Cb^r	Jacob Bertrand
pMBAD18G	Broad host range expression vector, pBAD promoter, Gm^r	Endoh and Engel (2009)
pJB142	PilG-HA in pMBAD18G, Gm^r	Bertrand (2010)
pJB100ΔfimV	Allelic exchange construct, ΔfimV in pJB100, Ap^r, Cb^r	This study
pYFI043	Allelic exchange construct, FimL-GFP in pJB100, Ap^r, Cb^r	Inclan *et al.* (2011)
pMBAD18G-GFP	pMBAD18G derivative, C-terminal GFP fusion vector, Gm^r	Endoh and Engel (2009)
pMBADFimV-GFP	pMBAD-GFP derivative to express FimL-GFP, Gm^r	This study
PaQa-reporter	PaQa reporter, PaQa-YFP, PrpoD-mKate2, Ap^r, Cb^r	Persat *et al.* (2015a)
mini-CTX-P*lac*p1-*lacZ*	*lacp1* promoter fused to *lacZ* in miniCTX, tet^r	Fulcher *et al.* (2010)
pkT25	BACTH vector to express N-terminal T25 fused protein, Km^r	Euromedex, Karimova *et al.* (2001)
pkNT25	BACTH vector to express C-terminal T25 fused protein, Km^r	Euromedex, Karimova *et al.* (2001)
pUT18C	BACTH vector to express N-terminal T18 fused protein, Ap^r	Euromedex, Karimova *et al.* (2001)
pUT18	BACTH vector to express C-terminal T18 fused protein, Ap^r	Euromedex, Karimova *et al.* (2001)
pkT25-zip	T25 fused N-terminal to a leucine zipper	Euromedex, Karimova *et al.* (1998)
pUT18C-zip	T18 fused N-terminal to a leucine zipper	Euromedex, Karimova *et al.* (1998)
pkT25-FimL	BACTH construct to express T25-FimL, Km^r	This study
pkNT25-FimL	BACTH construct to express FimL-T25, Km^r	This study
pUT18C-FimL	BACTH construct to express T18-FimL, Ap^r	This study
pUT18-FimL	BACTH construct to express FimL-T18, Ap^r	This study
pkT25-FimV	BACTH construct to express T25-FimV, Km^r	This study
pkNT25-FimV	BACTH construct to express FimV-T25, Km^r	This study
pUT18C-FimV	BACTH construct to express T18-FimV, Ap^r	This study
pUT18-FimV	BACTH construct to express FimV-T18, Ap^r	This study
pkT25-PilG	BACTH construct to express T25-PilG, Km^r	This study
pkNT25-PilG	BACTH construct to express PilG-T25, Km^r	This study
pUT18C-PilG	BACTH construct to express T18-PilG, Ap^r	This study

Table 1: *Continued*

Strain or plasmid	Genotype or relevant characteristic	Reference or source
pUT18-PilG	BACTH construct to express PilG-T18, Ap^r	This study
pkT25-$PilG_{D58A}$	BACTH construct to express T25-$PilG_{D58A}$, Km^r	This study
pkNT25-$PilG_{D58A}$	BACTH construct to express $PilG_{D58A}$-T25, Km^r	This study
pUT18C-$PilG_{D58A}$	BACTH construct to express T18-$PilG_{D58A}$, Ap^r	This study
pUT18-$PilGD_{58A}$	BACTH construct to express $PilG_{D58A}$-T18, Ap^r	This study
pkT25-PilH	BACTH construct to express T25-PilG, Km^r	This study
pkNT25-PilH	BACTH construct to express PilG-T25, Km^r	This study
pUT18C-PilH	BACTH construct to express T18-PilG, Ap^r	This study
pUT18-PilH	BACTH construct to express PilG-T18, Ap^r	This study

protocol with modifications. Briefly, overnight cultures were diluted 1/20 in M63 media. Cells were washed with M63 and OD_{600} of 0.6 in 100 μl in M63 media was added to 500 μl of Z-buffer (defined in the Euromedex manual). Fifty microliter chloroform and 25 μl 0.1% SDS was added to permeabilize cells with 10 s of vortexing. Samples were incubated at room temperature for 15 min. Fifty microliter of permeabilized cells was added to a 96-well plate and 50 μl of ONPG (*O*-nitrophenyl-β-D-galactoside) at 4 mg ml^{-1} was added to each well. After 20 min, 100 μl of 1 M Na_2CO_3 was added to each well and OD_{420} and OD_{550} were measured. β-galactosidase activity was calculated as Miller units = 1000 $(OD_{420} - 1.75 \times OD_{550})]/(T \times V \times OD_{600})$. Each combination was tested with three technical replicates and the experiment was performed 3 times.

Subsurface twitching motility stab assay

Plastic dishes (150 × 25 mm, Corning Product #430599) were filled with 50 ml LB 1% agar or VBM + Fe + 1% agar 1 day prior to the experiment. Prior to use, each plate was dried in a hood with lamellar air flow for at least 10 min to remove excessive moisture. Single colonies grown overnight on LB agar containing appropriate antibiotics were then stabbed with a p20 pipet tip to the agar plate interface. The plates were incubated at 37°C overnight in a humidified bag (plastic bag with a wet paper towel) for 24 h. The agar was scored around the edges with forceps and carefully removed and the resulting colony diameter was measured with a ruler. Each experiment was performed at least three times.

β-galactosidase assays

β-galactosidase activity was measured using a cAMP-dependent reporter fusion. The miniCTX-P*lacP1-lacZ* reporter (a kind gift of Dr. Matthew Wolfgang (Fulcher *et al.*, 2010)) was introduced into PAO1, PAO1Δ*vfr*, PAO1Δ*cyaB*, PAO1Δ*fimL*, PAO1Δ*fimV*, PAO1Δ*fimL*Δ*fimV* by allelic exchange by mating with S17-1. β-galactosidase assays were performed as described in the BACTH assay with the following modification. The cells were washed 3× with M63 media and resuspended to $OD_{600} = 0.4$. After cell permeabilization with chloroform and SDS, each sample was centrifuged for 10 min at 10,000 *g* to remove debris. Each experiment was performed five times with three technical replicates each time.

Surface Sensing

Surface sensing experiments were performed as previously described (Persat *et al.*, 2015a).

Fluorescence microscopy

Agar pads were prepared in 96-well glass bottom plates (in Vitro Scientific) by depositing 120 μl molten VBM + Fe media (3 g l^{-1} trisodium citrate, 2 g l^{-1} citric acid, 10 g l^{-1} K_2HPO_4, 3.5 g l^{-1} $NaNH_4PO_4{\bullet}4H_2O$, 1 mM $MgSO_4$, 18 μM $FeSO_4$) and 1% agarose into each well. For pPilG-GFP or pPilJ-GFP strains, 0.02% arabinose and 50 μg ml^{-1} gent was added to the molten agar pad solution. Ten minutes after pouring, a single colony was stabbed into each well and the plate was incubated at 37°C for 4 h. The bacteria were visualized with a CSU-X1 spinning disk confocal on a Nikon Eclipse Ti inverted microscope with an Andor Clara digital camera using Plan Apo 1.49 N.A. 100× Oil TIRF objective. Images were collected using differential interference contrast, 488 nm laser, and acquired with NIS-Elements software 4.10 (Nikon).

Phylogenetics and Bioinformatics. Bacterial species with TFP assembly genes (Fig. 6, shaded in orange) were selected based on representation of pilA, pilB, pilC, pilD, pilF, pilM, pilN, pilO, pilP, pilQ, pilT and pilU in the top 1000 blastp hits versus the NR database (excluding the Pseudomonas genus (taxid:286)) for the PAO1 protein sequences on March 1st, 2015. The species shaded in gray (Fig. 6) were selected for medical relevance and interest. The presence of each of 24 proteins (TFP assembly, chemotaxis and additional proteins) in each species was tested by pairwise tblastn of all proteins against the whole genome sequence of the given species using default options (Altschul, 1990 #6754). Significant alignments (*e*-value of less than 0.1) were manually reviewed for domains using HHPred and blastp (Soding, 2005 #6755). For the Chp chemosensory genes, a more stringent tblantn cut-off (e^{-50}) was used followed by HHPred and blastp to eliminate more distantly related chemotaxis homologs. Clustering of genes in in the chromosome was curated by visual inspection of tblastn hits. Complete 16S sequences for each species

were aligned by MUSCLE and phylogeny was generated by MrBayes. Accessions available on request.

Statistical analysis. Statistical analysis was performed using Graphpad Prism using ordinary one-way ANOVA and Tukey's multiple comparison posttest.

Acknowledgements

We thank Julia Chambers and Ryan Kaveh for technical assistance and members of the Engel lab for support. We thank Matthew Wolfgang (University of North Carolina, Chapel Hill) for the generous donation of the miniCTX-P_{lacp1}-*lacZ* reporter. This research was funded by grants for the NIH (AI42806, R56-AI065902; J.E.); the Gordon and Betty Moore foundation through Grant GBMF 2550.02 to the Life Sciences Research Foundation (A.P.); National Science Foundation Grant CBET-1330288 and NIH Pioneer Award DP1-AI-124669 (to Z.G.). The authors have no conflicts of interest to declare.

Author contributions

YI, AP, AG, JVD, NK, ZG and JE participated in the conception or design of the study. YI, AP, AG, JVD, JJ, NK, ZG and JE participated in the acquisition, analysis or interpretation of the data. YI, AP, AG, NK, ZG and JE participated in the writing of the manuscript.

References

Almblad, H., Harrison, J.J., Rybtke, M., Groizeleau, J., Givskov, M., Parsek, M.R., and Tolker-Nielsen, T. (2015) The cyclic AMP-Vfr signaling pathway in *Pseudomonas aeruginosa* is inhibited by cyclic Di-GMP. *J Bacteriol* **197**: 2190–2200.

Baker, M.D., Wolanin, P.M., and Stock, J.B. (2006) Signal transduction in bacterial chemotaxis. *Bioessays* **28**: 9–22.

Battesti, A., and Bouveret, E. (2012) The bacterial two-hybrid system based on adenylate cyclase reconstitution in *Escherichia coli*. *Methods* **58**: 325–334.

Beaussart, A., Baker, A.E., Kuchma, S.L., El-Kirat-Chatel, S., O'Toole, G.A., and Dufrene, Y.F. (2014) Nanoscale adhesion forces of *Pseudomonas aeruginosa* type IV Pili. *ACS Nano* **8**: 10723–10733.

Belas, R. (2014) Biofilms, flagella, and mechanosensing of surfaces by bacteria. *Trends Microbiol* **22**: 517–527.

Bertrand, J. (2010) *Genetic Analysis of the Chp Chemosensory System of Pseudomonas aeruginosa*. San Francisco: University of Californnia.

Bertrand, J.J., West, J.T., and Engel, J.N. (2010) Genetic analysis of the regulation of type IV pilus function by the Chp chemosensory system of *Pseudomonas aeruginosa*. *J Bacteriol* **192**: 994–1010.

Chiang, P., Habash, M., and Burrows, L.L. (2005) Disparate subcellular localization patterns of *Pseudomonas aeruginosa* Type IV pilus ATPases involved in twitching motility. *J Bacteriol* **187**: 829–839.

Chung, C.T., Niemela, S.L., and Miller, R.H. (1989) One-step preparation of competent *Escherichia coli*: transformation and storage of bacterial cells in the same solution. *Proc Natl Acad Sci USA* **86**: 2172–2175.

Coggan, K.A., and Wolfgang, M.C. (2012) Global regulatory pathways and cross-talk control *Pseudomonas aeruginosa* environmental lifestyle and virulence phenotype. *Curr Issues Mol Biol* **14**: 47–70.

Comolli, J.C., Hauser, A.R., Waite, L., Whitchurch, C.B., Mattick, J.S., and Engel, J.N. (1999) *Pseudomonas aeruginosa* gene products PilT and PilU are required for cytotoxicity in vitro and virulence in a mouse model of acute pneumonia. *Infect Immun* **67**: 3625–3630.

Endoh, T., and Engel, J.N. (2009) CbpA: a polarly localized novel cyclic AMP-binding protein in *Pseudomonas aeruginosa*. *J Bacteriol* **191**: 7193–7205.

Fields, S., and Song, O.-K. (1989) A novel genetic system to detect protein-protein interactions. *Nature* **340**: 245–246.

Filloux, A., and Ventre, I. (2006) [Two sensors to control bacterial life style: the choice between chronic or acute infection]. *Med Sci (Paris)* **22**: 811–814.

Frieden, T., (2013) ANTIBIOTIC RESISTANCE THREATS in the United States, 2013. In. http://www.cdc.gov/drugresistance/threat-report-2013/, pp. 69-70.

Fulcher, N.B., P.M. Holliday, E. Klem, M.J. Cann & M.C. Wolfgang, (2010) The Pseudomonas aeruginosa Chp chemosensory system regulates intracellular cAMP levels by modulating adenylate cyclase activity. *Molecular microbiology* **76**: 889–904.

Georgiadou, M., Castagnini, M., Karimova, G., Ladant, D., and Pelicic, V. (2012) Large-scale study of the interactions between proteins involved in type IV pilus biology in *Neisseria meningitidis*: characterization of a subcomplex involved in pilus assembly. *Mol Microbiol* **84**: 857–873.

Hall-Stoodley, L., and Stoodley, P. (2009) Evolving concepts in biofilm infections. *Cell Microbiol* **11**: 1034–1043.

Hall-Stoodley, L., Stoodley, P., Kathju, S., Hoiby, N., Moser, C., Costerton, J.W., Moter, A., and Bjarnsholt, T. (2012) Towards diagnostic guidelines for biofilm-associated infections. *FEMS Immunol Med Microbiol* **65**: 127–145.

He, K., and Bauer, C.E. (2014) Chemosensory signaling systems that control bacterial survival. *Trends Microbiol* **22**: 389–398.

Herzog, F., Kahraman, A., Boehringer, D., Mak, R., Bracher, A., Walzthoeni, T., Leitner, A., *et al.* (2012) Structural probing of a protein phosphatase 2A network by chemical cross-linking and mass spectrometry. *Science* **337**: 1348–1352.

Hoang, T.T., Kutchma, A.J., Becher, A., and Schweizer, H.P. (2000) Integration-proficient plasmids for *Pseudomonas aeruginosa*: site-specific integration and use for engineering of reporter and expression strains. *Plasmid* **43**: 59–72.

Holloway, B.W., and Morgan, A.F. (1986) Genome organization in Pseudomonas. *Ann Rev Microbiol* **40**: 79–105.

Inclan, Y.F., Huseby, M.J., and Engel, J.N. (2011) FimL regulates cAMP synthesis in *Pseudomonas aeruginosa*. *PloS One* **6**: e15867.

Jager, S., Gulbahce, N., Cimermancic, P., Kane, J., He, N., Chou, S., *et al.* (2011) Purification and characterization of HIV-human protein complexes. *Methods* **53**: 13–19.

Jager, S., Cimermancic, P., Gulbahce, N., Johnson, J.R., McGovern, K.E., Clarke, S.C., *et al.* (2012) Global landscape of HIV-human protein complexes. *Nature* **481**: 365–370.

Karimova, G., Pidoux, J., Ullmann, A., and Ladant, D. (1998) A bacterial two-hybrid system based on a reconstituted signal transduction pathway. *Proc Natl Acad Sci USA* **95**: 5752–5756.

Karimova, G., Ullmann, A., and Ladant, D. (2001) Protein-protein interaction between *Bacillus stearothermophilus* tyrosyl-tRNA synthetase subdomains revealed by a bacterial two-hybrid system. *J Mol Microbiol Biotechnol* **3**: 73–82.

Karimova, G., Dautin, N., and Ladant, D. (2005) Interaction network among *Escherichia coli* membrane proteins involved in cell division as revealed by bacterial two-hybrid analysis. *J Bacteriol* **187**: 2233–2243.

Leech, A.J., and Mattick, J.S. (2006) Effect of site-specific mutations in different phosphotransfer domains of the chemosensory protein ChpA on *Pseudomonas aeruginosa* motility. *J Bacteriol* **188**: 8479–8486.

Leighton, T.L., R. Buensuceso, P.L. Howell & L.L. Burrows , (2015) Biogenesis of Pseudomonas aeruginosa type IV pili and regulation of their function. *Environmental microbiology* **17**: 4148–4163.

Livermore, D.M. (2002) Multiple mechanisms of antimicrobial resistance in *Pseudomonas aeruginosa*: our worst nightmare? *Clin Infect Dis* **34**: 634–640.

Luo, Y., K. Zhao, A.E. Baker, S.L. Kuchma, K.A. Coggan, M.C. Wolfgang, G.C. Wong & G.A. O'Toole, (2015) A hierarchical cascade of second messengers regulates Pseudomonas aeruginosa surface behaviors. *mBio* **6**: 127–137.

Mandell, G.L., Bennett, J.E., and Dolin, R. (2010) *Mandell, Douglas, and Bennett's Principles and Practice of Infectious Diseases*. Philadelphia, PA: Churchill Livingstone/Elsevier.

Mirrashidi, K.M., Elwell, C.A., Verschueren, E., Johnson, J.R., Frando, A., Von Dollen, J., *et al.* (2015) Global mapping of the Inc-Human interactome reveals that retromer restricts Chlamydia infection. *Cell Host Microbe* **18**: 109–121.

Navare, A.T., Chavez, J.D., Zheng, C., Weisbrod, C.R., Eng, J.K., Siehnel, R., *et al.* (2015) Probing the protein interaction network of *Pseudomonas aeruginosa* cells by chemical cross-linking mass spectrometry. *Structure* **23**: 762–773.

Nicas, T.I., and Iglewski, B.H. (1984) Isolation and characterization of transposon-induced mutants of *Pseudomonas aeruginosa* deficient in production of exoenzyme S. *Infect Immun* **45**: 470–474.

Persat, A., Inclan, Y.F., Engel, J.N., Stone, H.A., and Gitai, Z. (2015a) Type IV pili mechanochemically regulate virulence factors in *Pseudomonas aeruginosa*. *Proc Natl Acad Sci USA* **112**: 7563–7568.

Persat, A., Nadell, C.D., Kim, M.K., Ingremeau, F., Siryaporn, A., Drescher, K., *et al.* (2015b) The mechanical world of bacteria. *Cell* **161**: 988–997.

Rossmann, F., S. Brenzinger, C. Knauer, A.K. Dorrich, S. Bubendorfer, U. Ruppert, G. Bange & K.M. Thormann, (2015) The role of FlhF and HubP as polar landmark proteins in Shewanella putrefaciens CN-32. *Molecular microbiology* **98**: 727–742.

Schweizer, H.P. (1992) Allelic exchange in *Pseudomonas aeruginosa* using novel ColE1-type vectors and a family of cassettes containing a portable *oriT* and the counter-selectable *Bacillus subtilis sacB* marker. *Mol Microbiol* **6**: 1195–1204.

Silby, M.W., Winstanley, C., Godfrey, S.A., Levy, S.B., and Jackson, R.W. (2011) Pseudomonas genomes: diverse and adaptable. *FEMS Microbiol Rev* **35**: 652–680.

Simon, R., Priefer, U., and Puhler, A. (1983) A broad host range mobilization system for in vivo genetic engineering: transposon mutagenesis in gram negative bacteria. *Biotechnology* **1**: 784–791.

Sowa, M.E., Bennett, E.J., Gygi, S.P., and Harper, J.W. (2009) Defining the human deubiquitinating enzyme interaction landscape. *Cell* **138**: 389–403.

Tan, M.W., Rahme, L.G., Sternberg, J.A., Tompkins, R.G., and Ausubel, F.M. (1999) *Pseudomonas aeruginosa* killing of *Caenorhabditis elegans* used to identify *P. aeruginosa* virulence factors. *Proc Natl Acad Sci USA* **96**: 2408–2413.

Tolker-Nielsen, T., (2014) Pseudomonas aeruginosa biofilm infections: from molecular biofilm biology to new treatment possibilities. *Acta Pathologica Microbiologica et Immunologica Scandanavia* **122**: 1–51.

Verschueren, E., Von Dollen, J., Cimermancic, P., Gulbahce, N., Sali, A., and Krogan, N.J. (2015) Scoring large-scale affinity purification mass spectrometry datasets with MiST. *Curr Protoc Bioinformatics* **49**: 8. 19. 1-16.

Wehbi, H., Portillo, E., Harvey, H., Shimkoff, A.E., Scheurwater, E.M., Howell, P.L., and Burrows, L.L. (2011) The peptidoglycan-binding protein FimV promotes assembly of the *Pseudomonas aeruginosa* type IV pilus secretin. *J Bacteriol* **193**: 540–550.

West, S.E., Schweizer, H.P., Dall, C., Sample, A.K., and L.J. Runyen-Janecky, (1994) Construction of improved *Escherichia-Pseudomonas* shuttle vectors derived from pUC18/19 and sequence of the region required for their replication in *Pseudomonas aeruginosa*. *Gene* **148**: 81–86.

Whitchurch, C.B., Leech, A.J., Young, M.D., Kennedy, D., Sargent, J.L., Bertrand, J.J., *et al.* (2004) Characterization of a complex chemosensory signal transduction system which controls twitching motility in *Pseudomonas aeruginosa*. *Mol Microbiol* **52**: 873–893.

Whitchurch, C.B., Beatson, S.A., Comolli, J.C., Jakobsen, T., Sargent, J.L., Bertrand, J.J., *et al.* (2005) *Pseudomonas aeruginosa* fimL regulates multiple virulence functions by intersecting with Vfr-modulated pathways. *Mol Microbiol* **55**: 1357–1378.

Wolfgang, M.C., Lee, V.T., Gilmore, M.E., and Lory, S. (2003) Coordinate regulation of bacterial virulence genes by a novel adenylate cyclase-dependent signaling pathway. *Dev Cell* **4**: 253–263.

Yamaichi, Y., R. Bruckner, S. Ringgaard, A. Moll, D.E. Cameron, A. Briegel, G.J. Jensen, B.M. Davis & M.K. Waldor (2012) A multidomain hub anchors the chromosome segregation and chemotactic machinery to the bacterial pole. *Genes Dev* **26**: 2348–2360.

Supporting information

Additional supporting information may be found in the online version of this article at the publisher's web-site.